JOURNAL OF MATERIALS SCIENCE 29 (1994) 1584–1588

Physicochemical properties of ZrF_4–BaF_2–LnF_3 glasses (Ln=Y or rare-earth elements)

A. KONISHI, H. IZUMI, R. KANNO, Y. KAWAMOTO*
Department of Chemistry, Faculty of Science, Kobe University, Rokkodai, Nada, Kobe 657, Japan

The influence of lanthanoid fluorides on physicochemical properties of fluorozirconate glasses has been examined on $60ZrF_4 \cdot 30BaF_2 \cdot 10LnF_3$ glasses (Ln = Y, La, Ce, Pr, Nd, Sm, Eu, Gd, Tb, Dy, Er, Tm, Yb or Lu). Physicochemical properties such as ion packing, hardness, molecular refraction, thermal stability and fluoride-ion conduction have been evaluated on the glasses by the density, refractive index, differential thermal analysis, thermomechanical analysis, Vickers hardness and electrical conductivity measurements. The variation of these properties with lanthanoid species and the relationships between them have been discussed to characterize lanthanoid fluoride-containing fluorozirconate glasses.

1. Introduction

In fluorozirconate glasses, which were discovered by Poulain *et al.* in 1975 [1], BaF_2 is considered to be the best primary glass-modifier. One of the reasons is considered to be because the size of the Ba^{2+} ion is appropriate to facilitate glass-formation by matching the sizes of the Zr^{4+} and F^- ions. In fact, the glass-forming ability in the binary ZrF_4–BaF_2 system is not high enough to yield glasses of practical sizes. Thus, the preparation of ZrF_4–BaF_2 glasses with a few millimetres thickness is extremely difficult and is limited to a very narrow composition region. As secondary glass-modifiers, therefore, one or more additional fluorides are generally incorporated to obtain fluorozirconate glasses of practical sizes. For example, YF_3 and REF_3 (RE = rare-earth elements) are known to be effective secondary glass-modifiers [2–5]. Consequently, in the ZrF_4–BaF_2–(YF_3 or REF_3) systems, the glass-forming abilities are greatly improved to give thick and bulky glasses over fairly wide composition regions.

It is recognized that the lanthanoid contraction, the size of the trivalent rare-earth ions, $r_{RE^{3+}}$, changes successively from 0.1172 nm in La^{3+} to 0.1001 nm in Lu^{3+} with a 0.001–0.002 nm decrease for every additional atomic number. If the glass-forming abilities in fluorozirconate glass systems depend essentially on an appropriate combination of the ionic sizes of glass-constituents, it might be expected that glass-formation in the ZrF_4–BaF_2–REF_3 system will vary appreciably with the rare-earth species. In fact, the glass-forming regions found for the ZrF_4–BaF_2–REF_3 (RE = La, Nd or Gd) systems vary considerably [3–5].

Fluorozirconate glasses containing trivalent rare-earth ions may be used as various photonics materials, e.g. low transmission-loss optical fibres of glasses containing lanthanum or gadolinium (e.g. [6]), fibre lasers of glasses containing neodymium, holmium or erbium (e.g. [7]), upconversion devices of glasses containing neodymium, holmium, erbium or thulium (e.g. [8]), fibre amplifiers of glasses containing praseodymium (e.g. [9]), etc. In developing these photonics-functional fluorozirconate glasses, one important subject which should be clarified is the influence of incorporated rare-earth ions on the physicochemical properties of the glasses. Recently, Uhlherr *et al.* have examined the structure and stability of $60ZrF_4 \cdot 30BaF_2 \cdot 10REF_3$ glasses using a molecular dynamics computer simulation technique [10]. Except for this, there has been no systematic study on the physicochemical properties of fluorozirconate glasses containing a series of rare-earth elements.

In the present work, therefore, the characterization of fluozirconate glasses containing a series of lanthanoid fluorides was performed on a composition $60ZrF_4 \cdot 30BaF_2 \cdot 10LnF_3$ (Ln = Y or rare-earth elements). The physicochemical properties, such as ion packing density, F–F mean distance, hardness, molecular refraction, thermal stability and fluoride ion conduction of the glasses were evaluated from the density, refractive index, differential thermal analysis (DTA), thermomechanical analysis (TMA), Vickers hardness and electrical conductivity measurements. Then the correlation between these physicochemical properties and the Ln species was examined.

2. Experimental procedure and results

2.1. Glass preparation

The composition of the prepared glasses was $60ZrF_4 \cdot 30BaF_2 \cdot 10LnF_3$ (Ln = Y, La, Ce, Pr, Nd, Sm, Eu, Gd, Tb, Dy, Er, Tm, Yb or Lu). Ultra-pure

---

* Author to whom all correspondence should be addressed.

0022–2461

chemicals of the respective metal fluorides were employed as raw materials. About 4 g batches of the raw materials, with the addition of about 1 g $NH_4F \cdot HF$, were melted in platinum crucibles under an argon atmosphere. The melts were kept at 850–900 °C for about 20 min and then quenched in flat-plate forms by pressing them with two preheated brass plates. The obtained glasses were annealed at the respective glass transition temperatures determined by DTA analysis.

2.2. Density

The densities of $60ZrF_4 \cdot 30BaF_2 \cdot 10LnF_3$ glasses were measured by the Archimedean method, using CCl_4 as an immersion liquid. The obtained density values are given in Table I.

2.3. Refractive index

Refractive index measurements were made with an Abbe refractometer. The results are also given in Table I.

2.4. Thermal characteristics

Glass-transition temperatures, crystallization temperatures and liquidus temperatures were determined by DTA experiments using α-Al_2O_3 as the standard. On the other hand, thermal expansion coefficients were determined by TMA experiments using an SiO_2 glass as the standard. Both measurements were performed at a rising temperature rate of $10\ K\,min^{-1}$ under an argon atmosphere.

The respective values obtained may be found in Table I.

2.5. Vickers hardness

Vickers hardness measurements were carried out using a Vickers hardness tester under a $1\ kg\,mm^{-2}$ load and a 15 s loading time. The obtained hardness values are given in Table I.

2.6. Electrical conductivity

The experiment was carried out using an a.c. method with an LCZ meter. The measured frequency and temperature ranges were from 30–5×10^6 Hz and from 120–260 °C, respectively. The measurements were performed under an argon atmosphere using a three-probe technique with sputtered gold electrodes. Electrical conductivity values were obtained by complex impedance plots of the a.c. data.

The results are given in Table I.

3. Discussion

As mentioned in Section 1, Uhlherr *et al.* performed a molecular dynamics computer simulation study on $60ZrF_4 \cdot 30BaF_2 \cdot 10REF_3$ glasses (RE = rare-earth elements) and discussed the structure and stability of the glasses [10]. This glass composition is the same as that studied in the present work. Therefore, before discussing the present results, their findings are summarized here.

The most striking change in structure observed for the $60ZrF_4 \cdot 30BaF_2 \cdot 10REF_3$ glasses is the F^- coordination environment around RE^{3+}. The F^- coordination number decreases from about 9 in La^{3+} to about 8.3 in Lu^{3+}, leading an increase in the F^- coordination number around F^- from about 9.3 for the lanthanum glass to about 9.6 for the lutetium glass. On the other hand, the F^- coordination environments around Zr^{4+} and Ba^{2+} show no remarkable changes. In spite of the considerable change in glass structure with rare-earth species, all the glasses exhibit almost the same stabilities.

3.1. Ion packing density, F–F mean distance and Vickers hardness

For the $60ZrF_4 \cdot 30BaF_2 \cdot 10LnF_3$ (Ln = Y or rare-earth elements) glasses, the molecular volumes were obtained from the respective density values, and then the ion packing densities and F–F mean distances were calculated. In the calculation, ionic radii of Zr^{4+}

TABLE I Physicochemical properties of $60ZrF_4 \cdot 30BaF_2 \cdot 10LnF_3$ glasses (Ln = Y or rare-earth elements)

Ln	$r_{Ln^{3+}}$ (nm)	d ($g\,cm^{-3}$)	n_D	T_g (°C)	T_c (°C)	T_m (°C)	α ($10^{-7}\,cm^{-1}$)	H_v	$\log[\sigma_{200\,°C}\,(S\,cm^{-1})]$	ΔE ($kJ\,mol^{-1}$)	$\log[\sigma_0\,(S\,cm^{-1})]$
Lu	0.1001	4.845	1.521	319	370	536	173	236	− 5.46	72.1	2.50
Yb	0.1008	4.827	1.523	319	381	531	169	235	− 5.53	72.6	2.49
Tm	0.1020	4.784	1.524	319	384	541	166	245	− 5.48	73.4	2.62
Er	0.1033	4.797	1.525	321	392	544	178	241	− 5.51	73.0	2.55
Y	0.1040	4.559	1.519	314	397	539	168	236	− 5.42	72.8	2.62
Dy	0.1052	4.744	1.524	317	401	539	160	231	− 5.43	72.6	2.59
Tb	0.1063	4.750	1.524	316	395	541	174	239	− 5.45	73.0	2.61
Gd	0.1078	4.735	1.523	319	394	532	172	229	− 5.32	71.5	2.57
Eu	0.1087	4.717	1.530	312	392	535	188	228	− 5.37	73.0	2.69
Sm	0.1098	4.689	1.524	312	391	526	186	229	− 5.32	72.0	2.63
Nd	0.1123	4.674	1.528	317	395	528	170	236	− 5.33	71.9	2.61
Pr	0.1130	4.665	1.529	315	392	523	173	227	− 5.28	70.8	2.54
Ce	0.1150	4.661	1.527	313	389	522	193	220	− 5.20	70.9	2.63
La	0.1172	4.643	1.526	316	392	528	183	221	− 5.20	70.0	2.53

Notes: d, density at 25 °C; n_D, refractive index at 25 °C; T_g, glass transition temperature; T_c, crystallization temperature; T_m, liquidus temperature; α, linear thermal expansion coefficient; H_v, Vickers hardness; $\log\sigma_{200\,°C}$, electrical conductivity at 200 °C; ΔE, activation energy for conduction; $\log\sigma_0$, pre-exponential term.

(0.084 nm), Ba^{2+} (0.142 nm), F^- (0.133 nm) and Ln^{3+} (values given in Table I) were employed. The ion packing density and F–F mean distance values obtained are plotted against the ionic radii of Ln^{3+} in Figs 1 and 2, respectively. It can be seen from the figures that, with increasing ionic radius of Ln^{3+}, the ion packing density decreases from 63% to 62% and the F–F mean distance increases from 0.2635 nm to 0.2655 nm. These facts indicate that the structure of $60ZrF_4 \cdot 30BaF_2 \cdot 10LnF_3$ glasses becomes more open with larger Ln^{3+} ions, though the magnitude of the decrease is very slight.

It is notable that the ion packing density values of 62%–63% in the present glasses are appreciably high, compared with those in other glasses, e.g. an SiO_2 glass (51%), a $70SiO_2 \cdot 23Na_2O \cdot 7MgO$ glass (54%) and a BeF_2 glass (50%). This coincides with the general understanding that fluorozirconate glasses are composed of denser packing of the glass constituent ions due to both high fluoride-ion coordination numbers around the metal ions and the highly ionic bond character.

The Ln^{3+} dependence of Vickers hardness is shown in Fig. 3. The Vickers hardness value decreases with increasing ionic radius of Ln^{3+}, in accord with the Ln^{3+} dependence observed for ion packing density. Because no substantial changes in glass structure with the Ln^{3+} species are anticipated for the present glasses, the observed Ln^{3+} dependence may be explained both by a decrease in the Ln^{3+}–F^- bond strength and by a more open structure in glasses containing Ln^{3+} of larger ionic radii.

3.2. Molecular refraction

The molecular refraction, R, of $60ZrF_4 \cdot 30BaF_2 \cdot 10LnF_3$ glasses was calculated from the measured refractive index and density values according to the Lorentz–Lorenz equation, $R = [(n^2 - 1)/(n^2 + 2)]V$ where V is the molecular volume.

As can be seen from Fig. 4, R increases almost linearly with increasing ionic radius of Ln^{3+}. This may be due to an increase in the ionic refraction of Ln^{3+} with increasing ionic radius of Ln^{3+}.

3.3. Thermal stability

One method of evaluating thermal stabilities of glasses is the Hrubý criterion in which thermal stability is expressed by the formula $(T_c - T_g)/(T_m - T_c)$ [11]. The thermal stabilities of $60ZrF_4 \cdot 30BaF_2 \cdot 10LnF_3$ glasses were evaluated using this criterion. Fig. 5 shows the dependence of thermal stability on the Ln^{3+} species, indicating that the thermal stability increases from about 0.3 to about 0.6 with increasing ionic radius of Ln^{3+}. Low thermal stabilities of glasses containing the Lu^{3+}, Yb^{3+}, Tm^{3+} and Er^{3+} ions may be attributable to both the low crystallization temperatures and the high liquidus temperatures.

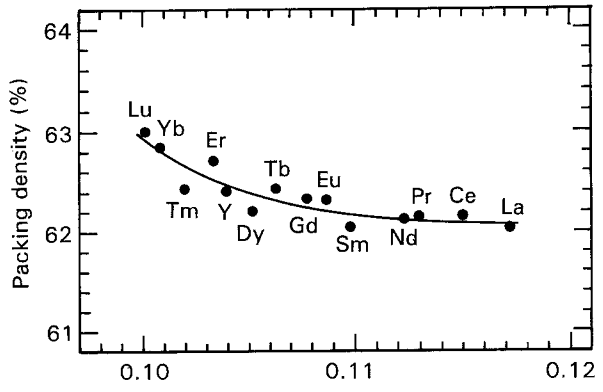

Figure 1 Packing densities of $60ZrF_4 \cdot 30BaF_2 \cdot 10LnF_3$ glasses (Ln = Y or rare-earth elements).

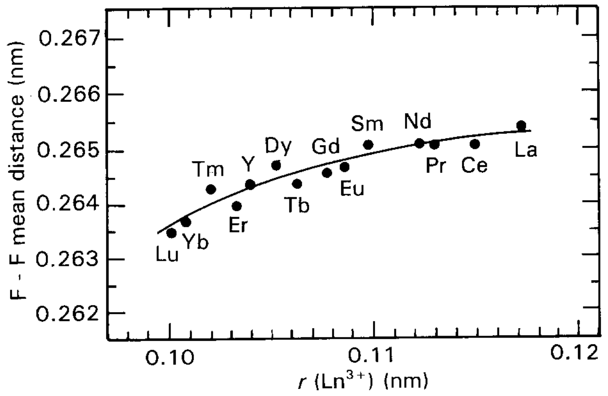

Figure 2 F–F mean distances in $60ZrF_4 \cdot 30BaF_2 \cdot 10LnF_3$ glasses (Ln = Y or rare-earth elements).

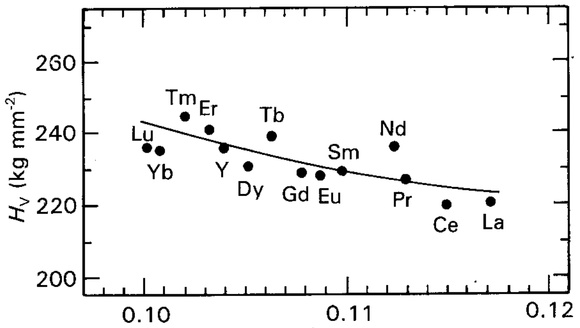

Figure 3 Vickers hardness of $60ZrF_4 \cdot 30BaF_2 \cdot 10LnF_3$ glasses (Ln = Y or rare-earth elements).

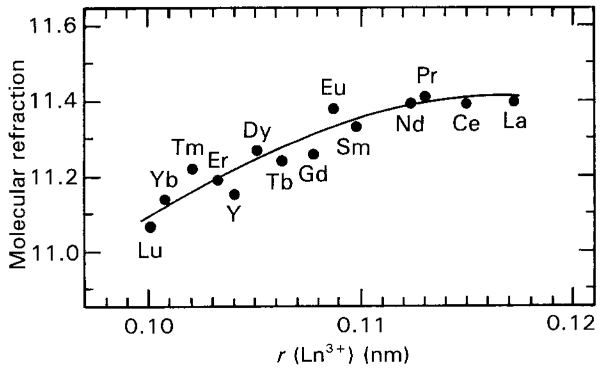

Figure 4 Molecular refraction of $60ZrF_4 \cdot 30BaF_2 \cdot 10LnF_3$ glasses (Ln = Y or rare-earth elements).

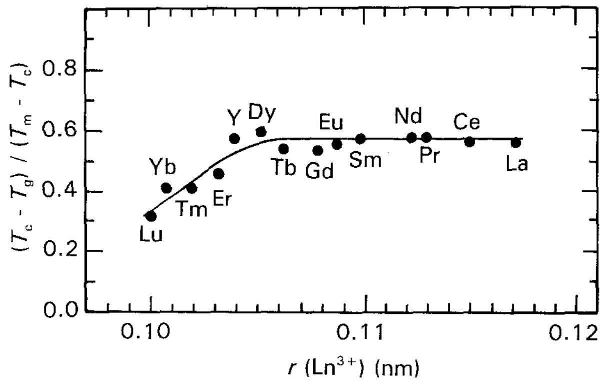

Figure 5 Thermal stability of $60ZrF_4 \cdot 30BaF_2 \cdot 10LnF_3$ glasses (Ln = Y or rare-earth elements) represented by the Hrubý criterion.

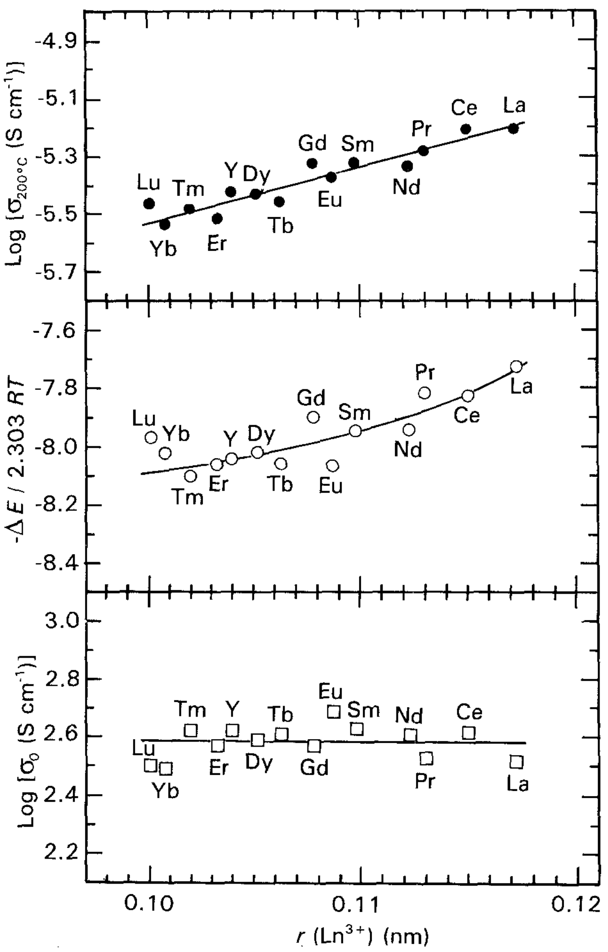

Figure 6 Electrical conductivities, activation energies for conduction and pre-exponential terms of $60ZrF_4 \cdot 30BaF_2 \cdot 10LnF_3$ glasses (Ln = Y or rare-earth elements).

3.4. Fluoride ion conduction

As is well known, the electrical conductivities of fluorozirconate glasses arise from fluoride-ion conduction, except for those of lithium fluoride-containing glasses which have mixed fluoride-ion and lithium-ion conduction [12]. Thus, the present electrical conductivity values are equivalent to the fluoride-ion conductivity values.

All the temperature dependences of electrical conductivities observed for $60ZrF_4 \cdot 30BaF_2 \cdot 10LnF_3$ glasses could be represented by an Arrhenius-type equation, $\log \sigma = \log \sigma_0 - \Delta E/2.303RT$. Fig. 6 shows $\log \sigma$ at 200 °C, $\log \sigma_0$ and $-\Delta E/2.303RT$ values which are plotted against the ionic radius of Ln^{3+}. In this figure the $-\Delta E/2.303RT$ value is adopted instead of ΔE, and also $\log \sigma_{200°C}$, $\log \sigma_0$ and $-\Delta E/2.303RT$ values are plotted on the ordinates with the same scale in order to facilitate comparison.

It can be seen from Fig. 6 that the $\log \sigma_{200°C}$ and $-\Delta E/2.303RT$ values increase almost linearly with increasing ionic radius of Ln^{3+}, while $\log \sigma_0$ changes little with the Ln^{3+} species. These facts indicate the following points: the fluoride ion conductivity is independent of the pre-exponential term and is determined by the activation energy term. Because an increase in $-\Delta E/2.303RT$ corresponds to a decrease in ΔE, the activation energy for fluoride-ion conduction decreases with increasing ionic radius of Ln^{3+}. This decrease in ΔE is deduced to be due partly to a decrease in the Ln^{3+}–F$^-$ bond strength with increasing ionic radius of Ln^{3+}.

4. Conclusion

The influence of lanthanoid ions on physicochemical properties of fluorozirconate glasses containing a series of lanthanoid fluorides was examined on $60ZrF_4 \cdot 30BaF_2 \cdot 10LnF_3$ glasses (Ln = Y, La, Ce, Pr, Nd, Sm, Eu, Gd, Tb, Dy, Er, Tm, Yb or Lu). The examined physicochemical properties were ion packing density, F–F mean distance, hardness, molecular refraction, thermal stability, thermal expansion coefficient and fluoride ion conductivity. All the properties changed remarkably with the Ln species. The F–F mean distance, molecular refraction, thermal stability, thermal expansion coefficient and fluoride-ion conductivity values increased with increasing ionic radius of Ln^{3+}. On the other hand, the ion packing density, and Vickers hardness values decreased with increasing ionic radius of Ln^{3+}. It is concluded that the main factors governing such Ln^{3+} dependences are the ionic radius of Ln^{3+} and the ionic bond strength between Ln^{3+}–F$^-$.

Acknowledgement

This work was supported partly by a Grant-in-Aid for Scientific Research (Priority Areas, New Functionality Materials – Design, Preparation and Control) from the Ministry of Education, Science and Culture (no. 04205100).

References

1. M. POULAIN, M. POULAIN and J. LUCAS, *Mater. Res. Bull.* **10** (1975) 243.
2. A. LECOQ and M. POULAIN, *J. Non-Cryst. Solids* **41** (1980) 209.
3. *Idem, ibid.* **34** (1979) 101.
4. J. LUCAS, M. CHANTHANASINH, M. POULAIN, M. POULAIN, P. BRUN and M. J. WEBER, *ibid.* **27** (1978) 273.
5. S. MITACHI and T. MANABE, *Jpn J. Appl. Phys.* **19** (1980) L313.
6. S. MITACHI, S. SHIBATA and T. MANABE, *Electron. Lett.* **17** (1981) 128.

7. M. C. BRIERLEY and P. W. FRANCE, *ibid.* **23** (1987) 815.
8. M. TAKAHASHI, R. KANNO, Y. KAWAMOTO, S. TANABE and K. HIRAO, *J. Non-Cryst. Solids*, accepted.
9. Y. OHISHI, T. KANAMORI, T. KITAGAWA, S. TAKAHASHI, E. SNITZER and G. H. SIGEL Jr, *Optics Lett.* **16** (1991) 1747.
10. A. UHLHERR, D. R. MACFARLANE, L. J. MOORE and P. D. THOMAS, in "Extended Abstracts of the 6th International Symposium on Halide Glasses", Clausthal, Germany, October 1989, p. 465.
11. A HRUBÝ, *Czech J. Phys.* **B22** (1972) 1187.
12. Y. KAWAMOTO, J. FUJIWARA and C. ICHIMURA, *J. Non-Cryst. Solids* **111** (1989) 245.

Received 26 January
and accepted 21 September 1993